

# Strongly correlated properties of the thermoelectric cobalt oxide $\text{Ca}_3\text{Co}_4\text{O}_9$

P. Limelette,<sup>1</sup> V. Hardy,<sup>1</sup> P. Auban-Senzier,<sup>2</sup> D. Jérôme,<sup>2</sup> D. Flahaut,<sup>1</sup> S. Hébert,<sup>1</sup> R. Frésard,<sup>1</sup> Ch. Simon,<sup>1</sup> J. Noudem,<sup>1</sup> and A. Maignan<sup>1</sup>

<sup>1</sup>Laboratoire CRISMAT, UMR 6508 CNRS-ENSICAEN et Université de Caen, 6, Boulevard du Maréchal Juin, 14050 CAEN Cedex, France

<sup>2</sup>Laboratoire de Physique des Solides (CNRS, U.R.A. 8502), Bâtiment 510, Université de Paris-Sud, 91405 Orsay, France

(Received 14 February 2005; published 30 June 2005)

We have performed both in-plane resistivity, Hall effect, and specific heat measurements on the thermoelectric cobalt oxide  $\text{Ca}_3\text{Co}_4\text{O}_9$ . Four distinct transport regimes are found as a function of temperature, corresponding to a low temperature insulating one up to  $T_{\min} \approx 63$  K, a strongly correlated Fermi liquid up to  $T^* \approx 140$  K, with  $\rho = \rho_0 + AT^2$  and  $A \approx 3.63 \times 10^{-2} \mu\Omega \text{ cm/K}^2$ , followed by an incoherent metal with  $k_F l \leq 1$  and a high temperature insulator above  $T^{**} \approx 510$  K. The specific heat Sommerfeld coefficient  $\gamma = 93 \text{ mJ}/(\text{mol K}^2)$  confirms a rather large value of the electronic effective mass and fulfils the Kadowaki-Woods ratio  $A/\gamma^2 \approx 0.45 \times 10^{-5} \mu\Omega \text{ cm K}^2/(\text{mJ}^2 \text{ mol}^{-2})$ . Resistivity measurements under pressure reveal a decrease of the Fermi liquid transport coefficient  $A$  with an increase of  $T^*$  as a function of pressure while the product  $A(T^*)^2/b_2$  remains constant and of order  $\hbar/e^2$ . Both thermodynamic and transport properties suggest a strong renormalization of the quasiparticles coherence scale of order  $T^*$  that seems to govern also thermopower.

DOI: 10.1103/PhysRevB.71.233108

PACS number(s): 71.27.+a, 72.15.-v, 65.40.Ba

While the discovery of superconductivity in hydrated  $\text{Na}_{0.35}\text{CoO}_2$  (Ref. 1) has considerably stimulated both experimental<sup>2</sup> and theoretical studies of layered cobalt oxides, the origin of their large thermopower coexisting with metallic properties<sup>3</sup> remains unclear. Of major interest for saving energy, thermoelectricity appears as a fundamental phenomenon whose mechanism can involve spin degeneracy,<sup>4</sup> charge frustration,<sup>5</sup> or enhanced effective mass in the vicinity of a Mott metal-insulator transition,<sup>6</sup> both combined with Coulomb repulsion. Thus, it is essential to demonstrate the existence of strong electronic correlations in cobalt oxides and to characterize their effects in order to put these scenarios to an experimental test. Derived from  $\text{Na}_x\text{CoO}_2$ , the cobaltite  $\text{Ca}_3\text{Co}_4\text{O}_9$  has a misfit structure consisting of a single  $[\text{CoO}_2]$  layer of  $\text{CdI}_2$ -type stacked with  $[\text{CoCa}_2\text{O}_3]$  rocksalt-type layers, with a different in-plane lattice parameter  $b$ .<sup>7,8</sup> As a result, this misfit-layered oxide shows highly anisotropic properties,<sup>7</sup> including magnetic ones at low temperatures.<sup>9</sup> Interestingly, while the  $\text{NaCo}_2\text{O}_4$  thermopower  $S$  increases continuously with temperature up to  $100 \mu\text{V/K}$  at 300 K,<sup>3</sup> the  $\text{Ca}_3\text{Co}_4\text{O}_9$  Seebeck coefficient becomes weakly temperature dependent from 150 K and reaches  $130 \mu\text{V/K}$  at 300 K.<sup>7</sup>

We report in this Brief Report on a detailed experimental study of both transport and thermodynamic properties of the misfit cobalt oxide  $\text{Ca}_3\text{Co}_4\text{O}_9$  to discuss whether or not strongly correlated features dominate and could explain a high thermopower. Temperature dependence of the in-plane single crystal resistivity from 2 to nearly 600 K has led us to identify transport crossovers, including a crossover from a Fermi liquid, with  $\rho = \rho_0 + AT^2$ , to an incoherent metal above  $T^*$ . This crossover has been analyzed from transport experiments under pressure within the range of 1 bar to 12 kbar below 300 K. By analyzing the pressure dependences of Fermi-liquid parameters, strong electronic correlations are confirmed.

Specific heat measurements of sintered samples have allowed us to determine an enhanced electronic contribution with  $\gamma = 93 \text{ mJ}/(\text{mol K}^2)$ . A critical comparison between the Fermi-liquid transport coefficient  $A$  and the Sommerfeld coefficient is made with the well-known Kadowaki-Woods ratio  $A/\gamma^2$ .<sup>10</sup> Temperature-dependent Hall effect measurements have confirmed holelike charge carriers in agreement with the positive thermopower. Both  $\gamma$  and the coherence temperature  $T^*$  seem to govern and thus explain the unusually high thermopower observed at ambient temperature in this compound.

Whereas previous transport experiments<sup>7,11</sup> were restricted to a limited temperature range, the in-plane single crystal ( $1 \times 0.5 \times 0.01 \text{ mm}^3$ ) resistivity in Fig. 1 was measured from 2 to nearly 600 K using a standard four terminal method. One can distinguish from this highly nonmonotonic behavior four transport regimes with first a low-temperature insulatinglike behavior characterized by a decreasing resistivity down to a minimum defining a transport crossover at  $T_{\min} \approx 63$  K. At higher temperatures, resistivity exhibits metallic behavior with basically two regimes. Up to the temperature  $T^* \approx 142$  K, one identifies a Fermi-liquid regime with a resistivity varying as  $\rho = \rho_0 + AT^2$ , as shown in the inset of Fig. 1. With a magnitude of  $3.63 \times 10^{-2} \mu\Omega \text{ cm/K}^2$ ,  $A$  is comparable to the ones measured in heavy fermion compounds such as  $\text{CePd}_3$ , for example. Moreover, one has to stress that the temperature  $T^*$  corresponds roughly to the Mott limit  $k_F l = (\hbar/e^2)c/\rho \sim 1$ , with the Fermi wave vector  $k_F$  and  $l$  the mean free path ( $c = 1.08 \text{ nm}$ ).<sup>7</sup> Therefore,  $T^*$  can be interpreted as a crossover from a low-temperature Fermi liquid to an incoherent metal (or “bad metal”) as observed in the vicinity of a Mott transition.<sup>12</sup> Still metalliclike, resistivity in the incoherent regime increases with temperature up to  $T^{**} \approx 510$  K, where it displays a broad maximum from which the material behaves as an insulator.

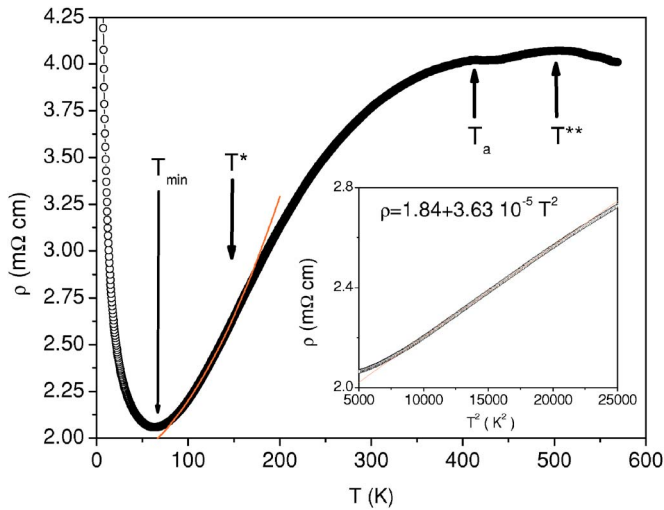


FIG. 1. (Color online) Temperature dependence of the in-plane single crystal resistivity. The three temperatures  $T_{min}$ ,  $T^*$ , and  $T^{**}$  separate, respectively, a low-temperature insulatinglike behavior, a strongly correlated Fermi liquid, an incoherent metal, and a high-temperature insulator, while  $T_a$  indicates an anomaly explained in the text. The inset displays  $\rho$  vs  $T^2$ .

Thus, one recovers the main features of strongly correlated systems near a Mott metal insulator transition observed experimentally in organic compounds<sup>12</sup> and predicted in the frame of the dynamical mean field theory<sup>13</sup> (DMFT). In this theoretical context, the density of states displays below the Fermi-liquid coherence scale  $T^*$  a well-formed quasiparticle peak, weakly temperature dependent. In that regime the resistivity obeys a Fermi-liquid  $T^2$  law. Above  $T^*$ , the quasiparticle resonance becomes strongly temperature dependent and the resistivity increases with  $T$ , reaching values exceeding the Mott limit associated to the bad or incoherent metal regime. Accordingly, the concept of a well-defined and long-lived quasiparticle loses its meaning in that regime, the depletion of the density of states corresponds to very short quasiparticle lifetime. At higher temperatures  $T \sim T^{**}$ , the quasiparticle resonance disappears altogether, leaving a pseudogap. In this third regime, the resistivity is that of an insulator with a decreasing behavior with temperature.<sup>12,13</sup>

Otherwise, we note in Fig. 1 an anomaly attributed<sup>7,11</sup> to spin-state transitions of the  $\text{Co}^{4+}$  and  $\text{Co}^{3+}$  ions appears at the temperature  $T_a \approx 400$  K. The fact that  $T_a$  differs from  $T^{**}$  by more than 100 K suggests that these two phenomena are probably not related to one another, although this calls for further more specific investigations.

As displayed in Fig. 2, transport experiments under hydrostatic pressure in a clamp cell have also been performed within the range of 6 to 12 kbar. A striking feature of this result is that by applying pressure the absolute value of the resistivity is increasing. Another effect of pressure is pointed out in the inset of Fig. 2 when plotting resistivity vs  $T^2$ , with a decrease of the slope  $A$  and an increase of the temperature range, i.e.,  $T^*$ , where  $\rho \sim T^2$ . Indeed, Fig. 3 confirms for all pressures investigated these two results with, respectively, the systematic decrease of the transport coefficient  $A$  while the coherence temperature  $T^*$  increases with pressure. Al-

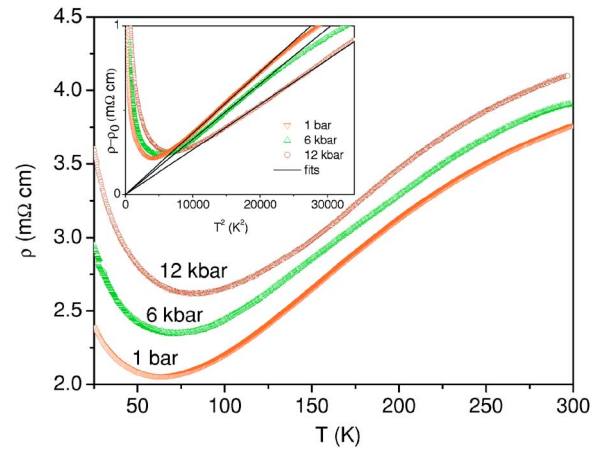


FIG. 2. (Color online) Temperature dependence of the in-plane resistivity under pressure, with, from the bottom to the top, 1 bar, 6 kbar, and 12 kbar (only three pressures are selected for clarity). The inset displays  $\rho - \rho_0$  vs  $T^2$  with the fitted lines.

ready experimentally observed in heavy fermions or near a Mott transition,<sup>12</sup> this quite *typical* strongly correlated Fermi-liquid behavior results basically from an increase of bandwidth due to pressure, and thus a decrease of the correlations that lowers the effective mass in contrast to quasiparticle coherence scale  $T^*$ .

An evidence for this interpretation is illustrated in Fig. 3 where the quantity  $A(T^*)^2/b_2$  is plotted as a function of pressure,  $b_2$  being the in-plane lattice parameter of the  $\text{CoO}_2$  subsystem.<sup>7</sup> Indeed, this product remains constant with pressure and of order  $\hbar/e^2$  within the range of 1 bar to 12 kbar, confirming that both  $A$  and  $T^*$  are efficient probes of electronic correlations. Besides, we note that this result is consistent with the DMFT picture of the Fermi liquid that predicts a key role of effective mass  $m^*$  with basically  $A \sim (m^*)^2$  and  $T^* \sim 1/m^*$ . We stress the fact that the pressure dependence of the lattice parameters is within the investi-

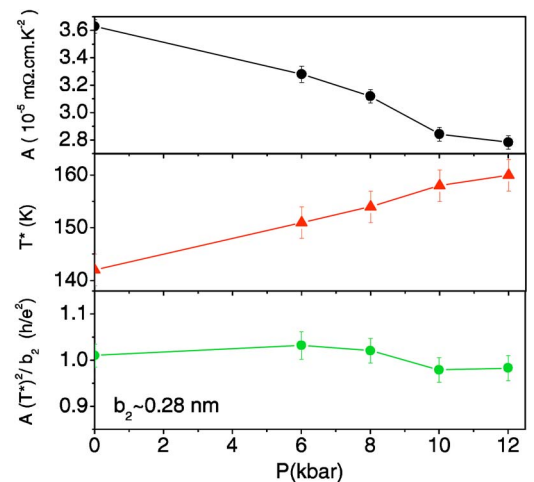


FIG. 3. (Color online) Pressure dependences of the Fermi liquid transport coefficient  $A$  (upper panel) and the coherence temperature  $T^*$  (middle panel). The lower panel exhibits the pressure independence of the product  $A(T^*)^2/b_2$  in unit of  $(\hbar/e^2)$ ,  $b_2$  being an in-plane lattice parameter.

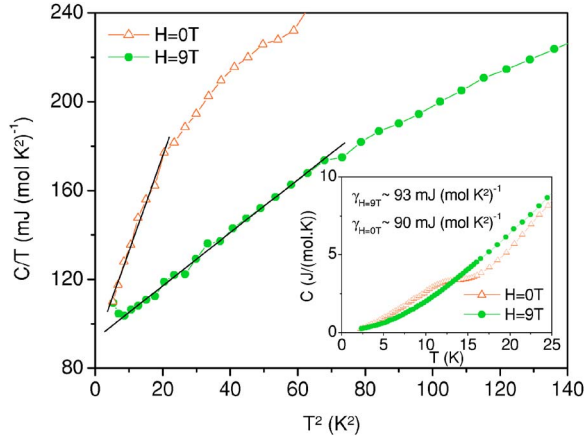


FIG. 4. (Color online) Temperature dependence of the specific heat for a sintered sample as  $C/T$  vs  $T^2$ . It's noteworthy that the 9-T magnetic field reveals the lattice contribution to the specific heat reducing a magnetic one (Ref. 9), and improve the quality of the determination of  $\gamma$ . The inset displays  $C$  vs  $T$ .

gated range of pressure negligible compared to the observed variation of  $A$  and  $T^*$ , thus ensuring a real correlation effect.

In order to check the renormalization of the Fermi liquid, implying a heavy electronic mass, we have performed specific heat experiments on a sintered sample. As observed in the inset of Fig. 4, specific heat exhibits a broad maximum below 20 K consistent with the presence of magnetic fluctuations observed in Ref. 9. Therefore, the specific heat has been measured under a 9-T magnetic field to quench magnetic fluctuations and reveal the  $T^3$  lattice contribution on an extended temperature range. In doing this, one obtains in Fig. 4 a specific heat behavior as  $C/T \sim \gamma + \beta T^2$  over the range 2–9 K with  $\gamma \approx 93$  mJ/(mol K<sup>2</sup>). One can emphasize the consistency between the latter value and the electronic contribution determined without the magnetic field (Fig. 4).

We stress here on the fact that the Fermi surface seems to remain unaffected down to the lowest temperatures since there is no signature of any phase transitions in both specific heat and thermopower measurements (Fig. 6). So, more than an order of magnitude higher than in conventional metals, the value of  $\gamma$  attests to a strong renormalization of Fermi-liquid parameters as the effective mass. Interestingly, the determined value is twice larger than in the NaCo<sub>2</sub>O<sub>4</sub> compound.<sup>14</sup> Consisting in a strong check of the previous conclusion, the comparison between transport and specific heat results with the so-called Kadowaki-Woods ratio gives  $A/\gamma^2 \approx 0.45 \times 10^{-5} \mu\Omega \text{ cm K}^2/(\text{mJ}^2 \text{ mol}^{-2})$ , in good agreement with the value found for heavy fermions.<sup>10</sup> Moreover, the experimental value of  $\gamma$  allows us to estimate the doping  $\delta \sim 0.32$  using the renormalized *free electron* expression  $\gamma = (\pi^2/2) \delta N_{av} k_B / T^*$ ,<sup>15</sup> with  $N_{av}$  the Avogadro number,  $k_B$  the Boltzmann constant, and  $T^*$  the determined quasiparticle coherence scale instead of the standard Fermi energy.

We have also performed single crystal Hall effect measurements as a function of temperature. We observe first in Fig. 5 a positive Hall resistance  $R_H$  in the full temperature range investigated, implying thus that charge carriers are holelike. Moreover,  $R_H$  exhibits globally a rather strong tem-

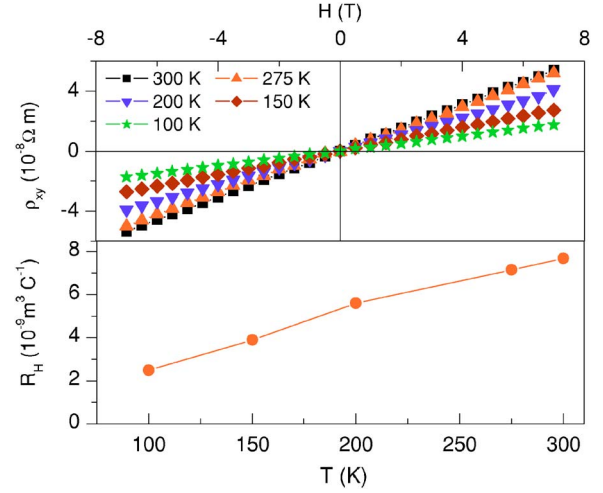


FIG. 5. (Color online) Magnetic-field dependence of the single crystal transverse resistivity for different temperatures (upper panel) and temperature dependence of Hall resistance (lower panel).

perature dependence from 100 up to 300 K, with an increase unusually large compared to conventional metals but consistent with the expected behavior of strongly correlated metals.<sup>16</sup>

Since both  $R_H$  and the thermopower  $S$  are positive, we can now discuss the influence of electronic correlations on thermoelectric properties in this compound. One may first emphasize that both  $S$  (see Fig. 6) and the figure of merit  $Z = S^2/(\rho\kappa)$  (Ref. 17) reach their maximum value at a temperature of order  $T^*$  ( $\kappa$  being the thermal conductivity). Therefore, Fig. 6 clearly displays that the temperature dependence of  $S$  up to  $T^*$  can be successfully described using a renormalized free electron thermopower  $S^*$  considering, as previously, the determined quasiparticle coherence scale  $T^*$  in Eq. (1), with  $q$  the elementary charge.

$$S^*(T) = \left( \frac{\pi^2}{6} \right) \frac{k_B T}{q T^*}. \quad (1)$$

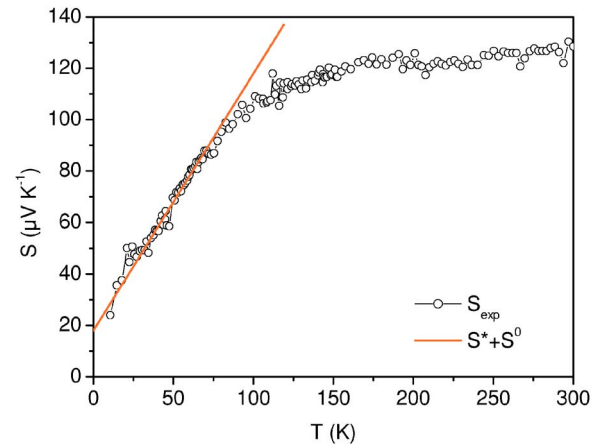


FIG. 6. (Color online) Temperature dependence of the single crystal thermopower  $S_{exp}$  (Ref. 7) compared to a renormalized free electron prediction  $S^*$  involving the quasiparticle coherence scale  $T^*$  (Fig. 1). Agreement is more apparent if a constant contribution  $S^0$  is added to  $S^*$ .

Due to the proportionality between  $S^*$  and the inverse of  $T^*$ , it follows from Eq. (1) and the pressure dependence of  $T^*$  that the low-temperature slope of  $S$  should decrease with pressure.

Furthermore, it appears on Fig. 6 that the agreement can be achieved up to nearly  $T^*/2$  when adding to  $S^*$  a low-temperature constant thermopower  $S^0 \approx 18 \mu\text{V/K}$ . Consequently, the thermopower  $S$  seems to result from the addition of two contributions including a constant one, namely,  $S^0$ , in the range of temperature investigated. While the origin of  $S^0$  requires further experimental work, the major contribution would in the present case come from strongly renormalized holelike carriers giving rise to a thermopower as  $S(T) \sim S^*(T) + S^0$  for  $T \ll T^*$ , and weakly temperature dependent for  $300 \text{ K} > T \gg T^*$ . One must finally emphasize the agreement between the low temperature thermopower ( $T \ll T^*$ ) and the coefficient  $\gamma$  with a doping  $\delta \sim 0.32$  following Eq. (2).<sup>15</sup>

$$S(T) = \left( \frac{\gamma}{3q\delta N_{av}} \right) T + S_0. \quad (2)$$

Reinforcing the interpretation of a high thermopower driven by electronic correlations, Eq. (2) confirms the key role of quasiparticle coherence scale  $T^*$ , or alternatively  $\gamma$ , in the electronic properties of this compound.

To conclude, both performed transport and thermodynamics measurements in the  $\text{Ca}_3\text{Co}_4\text{O}_9$  misfit cobalt oxide display quite unambiguously essential features of strongly correlated systems, as crossovers  $T^*$  and  $T^{**}$ , enhanced Fermi-liquid parameters  $A$  and  $\gamma$  fulfilling Kadowaki-Woods ratio, while typical pressure dependences of  $A$  and  $T^*$  are found. Furthermore, both experimental  $T^*$  and  $\gamma$  allow for a quantitative interpretation of the high thermopower governed by a strongly renormalized quasiparticles coherence scale of the order  $T^*$ . In order to test the renormalized thermopower prediction, we suggest that thermopower measurements under pressure in this compound would consist in a key experiment for a better understanding of thermoelectricity.

We are grateful to G. Kotliar for useful discussions.

- 
- <sup>1</sup>K. Takada, H. Sakurai, E. Takayama-Muromachi, F. Izumi, R. A. Dilanian, and T. Sasaki, *Nature (London)* **422**, 53 (2003).
  - <sup>2</sup>J. Sugiyama, J. H. Brewer, E. J. Ansaldo, H. Itahara, T. Tani, M. Mikami, Y. Mori, T. Sasaki, S. Hébert, and A. Maignan, *Phys. Rev. Lett.* **92**, 017602 (2004).
  - <sup>3</sup>I. Terasaki, Y. Sasago, and K. Uchinokura, *Phys. Rev. B* **56**, R12685 (1997).
  - <sup>4</sup>W. Koshibae, K. Tsutsui, and S. Maekawa, *Phys. Rev. B* **62**, 6869 (2000).
  - <sup>5</sup>O. I. Motrunich and P. A. Lee, *Phys. Rev. B* **69**, 214516 (2004).
  - <sup>6</sup>G. Pálsson and G. Kotliar, *Phys. Rev. Lett.* **80**, 4775 (1998).
  - <sup>7</sup>A. C. Masset, C. Michel, A. Maignan, M. Hervieu, O. Toulemonde, F. Studer, B. Raveau, and J. Hejtmanek, *Phys. Rev. B* **62**, 166 (2000).
  - <sup>8</sup>S. Lambert, H. Leligny, and D. Grebille, *J. Solid State Chem.* **160**, 322 (2001).
  - <sup>9</sup>J. Sugiyama, J. H. Brewer, E. J. Ansaldo, H. Itahara, K. Dohmae, Y. Seno, C. Xia, and T. Tani, *Phys. Rev. B* **68**, 134423 (2003).
  - <sup>10</sup>K. Kadowaki and S. B. Woods, *Solid State Commun.* **58**, 507 (1986).
  - <sup>11</sup>M. Shikano and R. Funahashi, *Appl. Phys. Lett.* **82**, 1851 (2003).
  - <sup>12</sup>P. Limelette, P. Wzietek, S. Florens, A. Georges, T. A. Costi, C. Pasquier, D. Jérôme, C. Mézière, and P. Batail, *Phys. Rev. Lett.* **91**, 016401 (2003).
  - <sup>13</sup>A. Georges, G. Kotliar, W. Krauth, and M. J. Rozenberg, *Rev. Mod. Phys.* **68**, 13 (1996).
  - <sup>14</sup>I. Terasaki, *Mater. Trans., JIM* **42**, 951 (2001).
  - <sup>15</sup>N. W. Ashcroft and N. D. Mermin, *Solid State Physics* (Holt-Saunders, Philadelphia, 1976).
  - <sup>16</sup>J. Merino and R. H. McKenzie, *Phys. Rev. B* **61**, 7996 (2000).
  - <sup>17</sup>K. Koumoto, I. Terasaki, and M. Murayama, *Oxide Thermoelectrics* (Research Signpost, India, 2002), p. 121.